9.3

VALIDATION OF THE CERES SHORTWAVE MEASUREMENTS OVER DESERT AND CLOUD SCENES

Chris Currey and Richard Green

NASA Langley Research Center,
Hampton, Virginia 23681-2199

1. INTRODUCTION

The Clouds and the Earth's Radiant Energy System (CERES) broadband shortwave channel, 0.3 - 5 μm, measures atmosphere and surface reflected solar radiation. CERES provides an in-flight tungsten lamp to monitor the shortwave radiometric stability over the lifetime of the instrument. Initial Tropical Rainfall Measurement Mission (TRMM) tungsten calibration results indicate a 0.6% change over the first six months of mission life (Priestley et al. 1998). The three channel intercomparison technique and the solar diffuser calibration results show shortwave stabilities of 0.2% and 0.3% for the same time period (Priestley et al. 1998). Current belief is that the tungsten lamp, not the radiometer, has drifted. Radiometers, optics, and onboard calibrators exposed to the harsh space environment often degrade. Independent validation studies based on bright Earth viewing measurements are necessary to support the in-flight filtered calibration results.

Instrument measurements of filtered radiances are converted to unfiltered radiances using the spectral correction algorithm (Green and Avis 1996). The spectral correction algorithm corrects for the imperfect spectral response of the instrument, thus providing an estimate of the solar radiance reflected back to space. Unfiltered radiances from different instruments may then be compared. This paper compares broadband shortwave results for CERES, Earth Radiation Budget Experiment (ERBE), and Scanning Radiometer for Radiation Budget (ScaRaB). ScaRaB data is from the Meteor 3 spacecraft (Mar. '94 - Feb. '95). Validation Earth targets provide a check of the spectral correction coefficients, and provide a means for cross-calibrating different datasets.

2. FORMULATION

Staylor (1993) used monthly clear-sky albedos from the Sahara desert (20°- 30°N, 0°- 30°E), to determine the stability of the first two years of ERBE shortwave data. Results have been extended to include ERBE data over the entire five year lifetime (Mar. '85 - Feb. '90). The monthly dispersion ($\sigma/\bar{x}$) is 3.4%. If we correct for seasonal variation, the monthly dispersion reduces to 1.0%. The CERES Sahara monthly albedos average 5.6% lower than the corresponding ERBE monthly albedos. Angular distribution models are used to convert unfiltered radiances to albedos. Shortwave anisotropy varies with solar zenith angle, viewing zenith angle, azimuth angle, scene type (e.g. ocean, land, and desert), and cloud condition (fraction, optical depth, particle size and phase). By restricting the data to nadir views only, we can compare different data sets without modeling the anisotropy. Results within the remainder of this paper are based on instantaneous nadir measurements.

Bright radiometrically stable desert targets (Rao et al. 1997), ice sheets (Loeb 1997), and clouds (Vermote and Kaufman 1995) have been used to calibrate instruments and monitor sensor degradation. Clear-sky isotropic albedo, or reflectance, is defined as

$$R = \frac{\pi I}{E_0 d^{-2} \cos\theta_0} \tag{1}$$

where, I is the unfiltered radiance ($Wm^{-2}sr^{-1}$) measured at the spacecraft, E_0 is the solar constant (1365 Wm^{-2}), θ_0 is the solar zenith angle, and d is the Earth-Sun distance in astronomical units (0.98 - 1.02).

In general, we will make use of the least squares regression $\tilde{y} = \hat{A} + \hat{B}\tilde{x}$, where $\tilde{y}$ is the estimate of reflectance at solar zenith $\tilde{x}$. This point estimate of reflectance calculated at $\tilde{x} = 40°$, referred to as $\hat{R}_{40}$, is the point of least variance. $\hat{R}_{40}$ is the primary statistic for target spatial and temporal testing as well as reflectance comparison from different instruments. The estimate of the variability about the regression line is

$$\sigma_\varepsilon^2 = \frac{1}{n-2}\sum_{i=1}^{\infty}(y_i - \hat{A} - \hat{B}x_i)^2 \tag{2}$$

and the point estimate variance is

$$\sigma_{\tilde{y}}^2 = \sigma_\varepsilon^2\left[\frac{1}{n} + \frac{(\tilde{x}-\bar{x})^2}{\sum(x_i-\bar{x})^2}\right]. \tag{3}$$

3. DESERT REFLECTANCE RESULTS

The Empty Quarter portion of the Saudi Desert (20°-22.5°N, 50° - 52.5°E), approximately 260 km by 280 km, consists mostly of sand dunes and sand seas. The lack of moisture and saline nature of the sand cause the region to be virtually free of vegetation. Clear nadir scenes are selected based on the ERBE scene identification algorithm. Figure 1 shows the reflectance for clear, partly cloudy, mostly cloudy, and overcast scenes

* *Corresponding author address*: Chris Currey, Mail Stop 423, NASA Langley Research Center, Hampton, Virginia 23681-2199; e-mail: j.c.currey@larc.nasa.gov.

for five years of ERBE data from the Earth Radiation Budget Satellite (ERBS). Clear is 0-5% cloud cover, and partly cloudy is 5-50% cloud cover. Misclassification between clear and partly cloudy is not considered a problem since there is minimal difference between reflectance regressions for $25° \le \theta_0 \le 52.5°$. Note the large increase in reflectance for mostly cloudy and overcast scenes. The Empty Quarter was clear 84% of the time; less than 5% of the scenes were mostly cloudy or overcast.

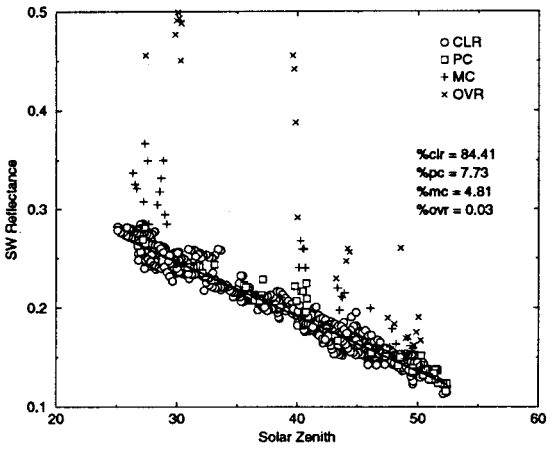

Figure 1: Sensitivity to Scene Identification

To determine the temporal stability of the Empty Quarter, scenes are segregated into four seasons. Nadir radiances are averaged for each satellite overpass. Seasonal estimates of $\hat{R}_{40}$ vary from 0.188 to 0.192. The maximum uncertainty of $\hat{R}_{40}$ from (3) is 1.4%, with Student's t tests revealing no significant statistical differences.

To determine spatial homogeneity, the Empty Quarter is subdivided into four 1.25° quadrants; overpass nadir radiances are averaged for each quadrant. Quadrant estimates of $\hat{R}_{40}$ vary from 0.187 to 0.193. The maximum quadrant uncertainty of $\hat{R}_{40}$ is 0.7%. Student's t tests show one quadrant (21.25° - 22.5°N, 51.25° - 52.5°E) to be significantly different than the other three quadrants. This quadrant is removed from further analysis.

The ERBE reflectance of the Empty Quarter is determined using all data from the three spatially uniform quadrants for $25° \le \theta_0 \le 52.5°$. $\hat{R}_{40}$ is 0.192, and from (3) the standard deviation is 0.4%. Using the same technique, eight months (Jan. '98 - Aug. '98) of CERES Empty Quarter measurements produce an $\hat{R}_{40}$ of 0.178 ±1.2%. Thus, CERES reflectance is 7% lower than ERBE, and statistically different. No attempt was made to calculate the point estimate reflectance using ScaRaB data due to an insufficient number of clear samples collected over the nine month dataset.

4. CLOUD REFLECTANCE RESULTS

Deep convective clouds are evaluated as validation targets for broadband shortwave data. Clouds, unlike deserts, are not limited to small uniform geographical regions. Reflectance is brighter and less susceptible to atmospheric scattering and absorption due to the high altitudes (>10 km). Measurement scenes are screened based on black body brightness temperature thresholds using Planck's law:

$$T_B = \frac{C_2}{\lambda \ln\left(1 + \frac{C_1}{\pi I_\lambda \lambda^5}\right)} \qquad (4)$$

where $C_1 = 3.74 \times 10^8\ \mathrm{W m^{-2}}$, $C_2 = 14387\ \mathrm{mK}$, λ denotes the wavelength interval, and I_λ represents the radiant energy emitted at the given temperature and wavelength. Filtered radiance thresholds for 205 K, 215 K, and 225 K are calculated by applying instrument spectral responses to the black body radiances and integrating over 8 - 12 μm, 5 - 100 μm, and 10.5 - 12.5 μm for the CERES, ERBE, and ScaRaB channels, respectively. To ensure independent sampling, reflectances are calculated per cloud system, which are typically separated by more than 1000 km. Cloud systems must contain two or more nadir measurements. They are sorted based on the standard deviation, or dispersion ($D = \sigma/\bar{x}$), of radiances within the system. Clouds over land and ocean are combined since no statistical difference in $\hat{R}_{40}$ was detected.

Table 1 presents the reflectance linear regressions for $\cos\theta_0$ over $0° \le \theta_0 \le 80°$. The number of cloud systems (n), point estimates ($\hat{R}_{40}$) with standard deviations in parentheses, and regression uncertainties (σ_ε) are calculated for each dispersion (D) and brightness temperature (T_B). ERBE cloud reflectances were calculated from four years of ERBS data (Jan. - Aug., '86 - '89). These dates were chosen to match the available CERES data. Cloud reflectance tends to increase as dispersion decreases. For the 205 K threshold, $\hat{R}_{40}$ increases from 0.7638 to 0.7755 as dispersion varies from 0.20 to 0.02. Reflectance also increases as temperature decreases. For $D \le 0.07$, reflectance increases from 0.6896 to 0.7671 as temperature decreases from 225 K to 205 K. The number of uniform clouds that meet each dispersion criteria decreases from 215 K to 225 K. Cloud systems with temperature thresholds less than 205 K have the lowest variability, $\sigma_\varepsilon < 0.03$, over the full solar zenith range $0° \le \theta_0 \le 80°$.

The temporal stability of bright uniform 205 K clouds ($D \le 0.04$), is determined by processing each year of ERBE data independently. Figure 2 shows the measured reflectance versus the $\cos\theta_0$ for each year. The mean yearly reflectance point estimate ($\hat{R}_{40}$) is 0.774 ±0.3%. The largest deviation of 0.5% occurs in 1988. We conclude that $\hat{R}_{40}$ for uniform cold clouds with $T_B \le 205$ K is extremely stable over time.

Table 1: ERBE Deep Convective Cloud Reflectance

Dispersion ≤ D	$T_B \leq 205$ K			$T_B \leq 215$ K			$T_B \leq 225$ K		
	n	$\hat{R}_{40}$ (σ)	σ_ε	n	$\hat{R}_{40}$ (σ)	σ_ε	n	$\hat{R}_{40}$ (σ)	σ_ε
.02	244	.7755 (.0018)	.0252	529	.7383 (.0016)	.0353	188	.6923 (.0035)	.0462
.03	349	.7738 (.0015)	.0257	934	.7362 (.0013)	.0359	349	.6952 (.0025)	.0438
.04	442	.7715 (.0014)	.0263	1339	.7347 (.0010)	.0354	515	.6943 (.0021)	.0446
.05	509	.7698 (.0014)	.0268	1758	.7324 (.0009)	.0352	693	.6933 (.0018)	.0444
.07	585	.7671 (.0013)	.0274	2464	.7287 (.0008)	.0351	1134	.6896 (.0014)	.0432
.10	624	.7657 (.0013)	.0282	2887	.7234 (.0008)	.0366	1726	.6856 (.0011)	.0412
.20	643	.7638 (.0014)	.0296	2887	.7203 (.0008)	.0379	2630	.6765 (.0008)	.0406

To compare reflectances from different instruments, CERES nadir field of view (FOV) 10 km measurements are averaged to match ERBE 40 km and ScaRaB 60 km nadir FOV sizes. For ERBE, this amounts to averaging two scans of 9 measurements each centered at nadir. For ScaRab we used a 3x13 average. Table 2 shows the final results comparing CERES, ERBE, and ScaRaB scanners. Increasing FOV size decreases the standard error (σ_ε), yet decreases the number of detected uniform clouds. Scans are averaged thus decreasing the number of available FOVs, and 10 km measurements within the enlarged FOV are required to be overcast. To exclude seasonal effects, ERBE and ScaRaB are limited to the same months as CERES. Reflectance is calculated for the solar zenith range $0° \leq \theta_0 \leq 80°$ and cloud dispersion $D \leq 0.07$. CERES 40 km point estimate reflectance ($\hat{R}_{40} = 0.7518 \pm 0.2\%$) is 2% darker than ERBE ($\hat{R}_{40} = 0.7671 \pm 0.2\%$). CERES 60 km point estimate reflectance ($\hat{R}_{40} = 0.7487 \pm 0.4\%$) is 4% darker than ScaRaB ($\hat{R}_{40} = 0.7762 \pm 0.4\%$).

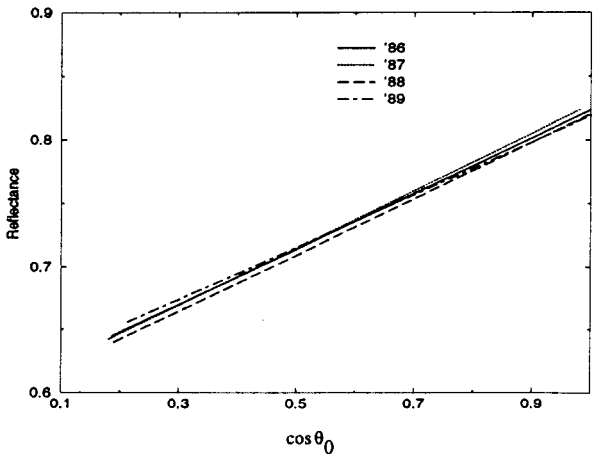

Figure 2: ERBE Cloud Reflectance Temporal Stability

5. SUMMARY

Earth targets have been identified for validation of the CERES broadband shortwave channel. Using five

Table 2. Reflectances for $T_B \leq 205$ K and $D \leq 0.07$

Instrument	Point Est. ($\hat{R}_{40}$)	Std Dev ($\sigma_{\hat{R}_{40}}$)	Number of Samples	σ_ε
CERES 10 km	.7479	.0016 (0.21%)	447	.0321 (4.3%)
CERES 40 km	.7518	.0017 (0.23%)	184	.0219 (2.9%)
ERBE	.7671	.0013 (0.17%)	585	.0274 (3.6%)
CERES 60 km	.7487	.0029 (0.39%)	79	.0213 (2.8%)
ScaRaB	.7762	.0031 (0.40%)	108	.0300 (3.9%)

years of ERBE scanner data, the Empty Quarter (2.5° region) within the Saudi Desert is spatially and temporally characterized. Empty Quarter reflectance for the first eight months of CERES is defined with a standard deviation of 1.2%. CERES desert reflectance is 7% lower than ERBE.

The desert as a calibration site is limited by its small size, possible greening, and overhead atmospheric scattering and absorption. These limitations are overcome with the coldest deep convective clouds. High bright clouds with temperatures less than 205 K are found to be numerous and consistent to define CERES reflectance with a standard deviation less than 0.4%. These clouds are 2% darker than ERBE, and 4% darker than ScaRaB. Measured radiances must be unfiltered with spectral correction coefficients based on pre-flight instrument calibration spectral responses. Uncertainties in the spectral correction process may account for the differences between CERES, ERBE, and ScaRaB. The fact that deserts and clouds give different results supports the possibility of a spectral problem.

6. ACKNOWLEDGEMENTS

The authors thank Martial Haeffelin for processing ScaRaB data, Stephanie Weckmann for processing CERES and ERBE monthly data, and Jean Philippe Duvel, ScaRaB Principal Investigator, for providing the ScaRaB data and window channel conversion routine.

7. REFERENCES

Green, R., L. Avis, 1996: Validation of ERBS Scanner Radiances, *J. Atmos. Ocean. Tech.*, **13**, 851-862.

Loeb, N., 1997: In-flight calibration of NOAA AVHRR visible and near-IR bands over Greenland and Antarctica, *Int. J. Remote Sens.*, **18**, 477-490.

Priestley, K., R. Lee, B. Barkstrom, S. Thomas, K. Thornhill, J. Paden, D. Pandey, R. Wilson, H. Bitting, and G. Smith, 1998: Radiometric stability of the CERES scanning thermistor bolometer radiometers, *Proc. SPIE*, **3439**, 303-310.

Rao, C. R., J. Chen, J. Sullivan, N. Zhang, and W. Wang, 1997: Vicarious calibration of meteorological satellite sensors in the visible and near-infrared regions of the spectrum, *Proc. SPIE*, **3117**, 320-331.

Staylor, F., 1993: Stability of the Earth Radiation Budget Experiment Scanner Results for the First Two Years of Multiple Satellite Operation, *J. Atmos. Ocean. Tech.*, **10**, 827-832.

Vermote, E., Y. Kaufman, 1995: Absolute calibration of AVHRR visible and near-infrared channels using ocean and cloud views, *Int. J. Remote Sens.*, **16**, 2317-2340.